ENCIT 2018

ABCM Associação Brasileira de Engenharia e Ciências Mecânicas

17th Brazilian Congress of Thermal Sciences and Engineering
November 25th-28th, 2018, Águas de Lindóia, SP, Brazil

ENCIT-2018-0816
EXPERIMENTAL ESTIMATION OF THE LOCATION AND INTENSITY OF A HEAT SOURCE FROM SURFACE TEMPERATURES USING THE SEQUENTIAL METHOD

Alisson Augusto Azevedo Figueiredo[1]
Jefferson Gomes do Nascimento[2]
Eduardo Peixoto de Oliveira[3]
Gilmar Guimarães[4]
Federal University of Uberlândia - School of Engineering, Campus Santa Mônica, Av. João Naves de Ávila, 2121, Uberlândia, Minas Gerais, Brazil
[1]alissonfigueiredo@hotmail.com, [2]jeffersongomes@ufu.br, [3]eduardopeixoto@ufu.br, [4]gguima@ufu.br

Abstract. *The aim of this work is to estimate the location and intensity of a heat source (tumor) within a tissue from surface temperatures using specified sequential function method. First, the 1D bioheat equation is solved analytically using Green's Functions method. Then, sequential method is used for the estimation of tumor heat generation and the Pearson correlation coefficient is used to determine the location of the heat source. Numerical results obtained from simulated temperatures in the commercial software COMSOL were accurate, i.e., the location and intensity of the tumor were estimated with errors less than 0.1%. Experimental results using a phantom tissue were satisfactory, i.e., the location and intensity of the tumor were estimated with errors less than 10%.*

Keywords: *Analytical solution, tumor, heat source, surface temperature, sequential method, experimental data.*

1. INTRODUCTION

As an object of study and curiosity since prehistory, our understanding of the human body continues to increase. One of the great ancient Greek philosophers, Hippocrates (460-370 BC), considered as the "father of medicine", believed that an increase in the innate human body temperature was the main signal for the diagnosis of a disease. Mud was spread on the patient, and the location where it dried and hardened first was observed. These observations were used as an indication of a pathology (Adams, 1849). Since then, research and clinical observations have shown that certain temperatures in the human body can indicate normal or abnormal physiological processes.

The first quantitative relationship describing energy transport in living tissues, including the effects of blood flow on tissue temperature (on an ongoing basis), was presented by Harry H. Pennes in 1948. The equation derived from this study, originally designed to predict the temperature field in the human forearm, is the most common representation of the spatial and temporal distribution of temperature in biological systems, and is called the "bioheat equation" or "Pennes' equation" (Pennes, 1948). Following Pennes' studies and the use of his equation in many biological systems, new models have been proposed to give a more realistic description of the bioheat transfer process (Mitchell and Myers, 1968; Keller and Seiler, 1971; Klinger, 1978; Chen and Holmes, 1980; Weinbaum and Jiji, 1985; Roetzel and Xuan, 1998; Nakayama and Kuwahara, 2008).

In 1956, Lawson found that the skin temperature in the region of breast cancer was higher than that of normal tissue. He also showed that venous blood draining from the malignant tumor is often warmer than that of the arterial system (Amalu *et al.*, 2006).

In recent years, the medical community has considered cancer diagnosis using skin surface temperature as an adjuvant method, i.e., it should be used alongside other established methods such as tomography, magnetic resonance imaging (MRI), and mammography (in the case of a breast tumor).

The International Academy of Clinical Thermology states that thermography can detect the initial stages of a cancer, but does not have the ability for tumor localization (of Clinical Thermology, 2017). The American Cancer Society says that thermography may be used to supplement information from other method and help identify cancers that are close to the skin. Still, thermography cannot find cancers that are deeper in the part and cannot detect small cancers (BreastCancer.org, 2017).

Thermography is still not considered self-sufficient, and another type of examination is necessary for a valid diagnosis of the disease. Several researches are working on techniques that make use of surface temperatures more effectively for

the detection of a tumor or other diseases.

Numerical studies pertaining to the simultaneous estimation of size, radial location, and angular location of a malignant tumor in a 3D human breast can be realized using the curve fitting method (Mishra and Das, 2015). Goughari et al. used *in vitro* intraoperative thermal imaging with artificial neural networks for the diagnosis and localization of brain (phantom tissue) tumors (Sadeghi-Goughari *et al.*, 2016). Bhowmik et al. employed a genetic algorithm and simulated annealing to characterize subsurface skin cancer features such as the tumor diameter, penetration depth, blood perfusion, and metabolic heat generation based on the thermal response of the skin surface obtained from thermal images simulated using a commercially available finite element solver, COMSOL Multiphysics (Bhowmik and Repaka, 2016). Experiments were conducted using a resistance heater embedded in agar to simulated the heat produced by a tumor in a biological tissue. The resulting temperature distribution on the surface was imaged using an infrared camera. To estimate the location and heat generation rate of the source from these temperature distributions, a genetic algorithm was used as the estimation method (Mital and Scott, 2006).

In this study, the inverse problem is developed from numerical simulations based on the sequential method coupled with linear correlations for estimating the location and intensity of a heat source ("tumor") in one-dimensional cases of a cancer. As imput data, only the surface temperatures are used.

2. CHARACTERISTCS OF TUMOR

Figure 1 shows the anatomy of the human skin, which is basically comprised of three layers: epidermis, dermis and fat layer. The melanocytes, cells where the melonama cancer type develop are between the first two layers.

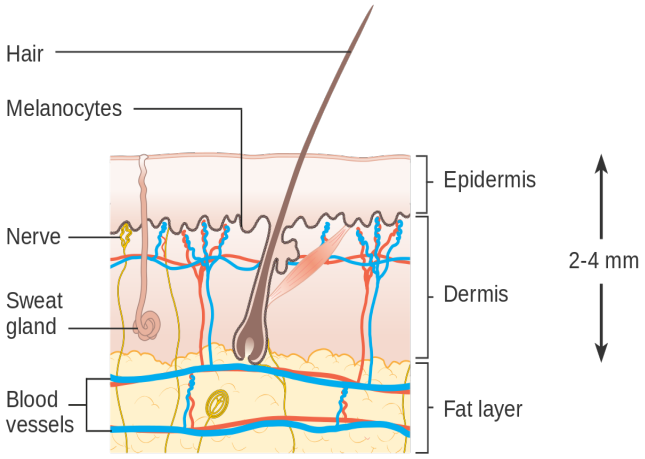

Figure 1. Internal structure of the breast (GenisisCare, 2018).

Skin cancers can occur on any part of the skin and can be divided into 3 main types which can be classified as 2 separate groups. Firstly, non-malignant melanoma skin cancer and secondly malignant melanoma skin cancer. Non malignant melanoma skin cancers arise in the upper layers of the skin and are extremely common, 74% of these are basal cell carcinomas (sometimes referred to as rodent ulcers), 23% are squamous cell carcinomas and the other 3% are a mixed group of rare skin cancers. They are more than 102,000 new cases registered each year in the UK, but exact numbers are difficult to assess as it is estimated that approximately 30-50% of basal cell carcinomas (BCC) and 30% of squamous cell carcinomas (SCC) are not entered onto the cancer register. Higher incidence in men, male to female ratio is 13:10. Age related, incidence rises from 40 years of age and peaks in the 70+ age group (GenisisCare, 2018).

Melanoma is the 5th most common cancer in the UK. Overall slightly higher incidence in females, male to female ratio approximately 10:11. In the 20-24 year age group the male to female ratio is 4:10 but from 60 years of age it is higher in men i.e. 11:10 in the 60-64years age group and 17:10 in those aged 85+ years. Incidence rises steadily from the age of 20 years and the number of cases diagnosed each year is increasing. Risk factors are sun exposure and sunbeds (ultra violet radiation) particularly in Caucasians, 86% of cases are linked to UVR exposure. Also, a family history of malignant melanoma, particularly if one or more relatives were diagnosed at under 30 years of age, large number of moles (100+), previous malignant melanoma, Crohn's disease and ulcerative colitis, HIV and AIDS infection. Also, some occupational exposure to coal tar pitch, soot, mineral oils, arsenic and possibly creosotes and petroleum refining (GenisisCare, 2018).

In both cases sympthoms can include: BCC, non-healing scaly area of skin, smooth lump with a 'pearly' appearance, non-healing area of skin that may have a hard, crusty surface that is sometimes tender and may bleed (GenisisCare, 2018).

Examinations based on images to aid diagnosis of breast diseases and other types of cancer can be classified as structural and functional. Structural exams allow the visualization of the internal structures of the breast, e.g., mammography,

ultrasound, and MRI scans. Functional exams allow the visualization of the functioning of the organs and the flow of liquids, e.g., ultrasound, MRI and thermography (Bezerra *et al.*, 2013).

This work is intended to assist the early detection of cancer using temperatures on the surface of the skin in one-dimensional cases. To reach this objective, it is necessary to understand the heat transfer phenomenon in living tissues based on the bioheat equation.

3. BIOHEAT EQUATION

Heat transfer in living organisms can be characterized using Eq. (3), also known as Pennes' equation (Pennes, 1948):

$$k\frac{\partial^2 T}{\partial x^2} + k\frac{\partial^2 T}{\partial y^2} + k\frac{\partial^2 T}{\partial z^2} + Q_p + Q_m + Q_e = \rho c\frac{\partial T}{\partial t} \tag{1}$$

where Q_p is the source of heat due to blood perfusion, Q_m is the volumetric metabolic heat generation, and Q_e is related to an external source of heat.

The source of heat due to blood perfusion (Q_p) is characterized by convective heat transfer effected by the blood through the capillary vascularization present in living tissue, which is proportional to the temperature difference between arterial blood entering the tissue and venous blood exiting the tissue (Charny, 1992). This term is given by

$$Q_p = w\rho_s c_s(T_a - T) \tag{2}$$

where w is blood flow rate [1/s], ρ_s is the specific mass of blood [kg/m^3], c_s is the specific heat of blood [J/(kg K)], T_a is the arterial blood temperature $\left[^{\mathrm{o}}\mathrm{C}\right]$, and T is the temperature of the tissue $\left[^{\mathrm{o}}\mathrm{C}\right]$.

4. ONE-DIMENSIONAL ANALYTICAL SOLUTION

Figure 2 shows the 1D model used to obtain the solution of Pennes' equation. The biothermic 1D problem to be analyzed should represent heat transfer in human tissue, simulating a body composed of layers of normal (healthy) tissues and a layer with a tumor. The 1D model can provides initial information about heat transfer in the tissue and improves the efficiency of the technique developed for the inverse problem. In this model, one surface is exposed to a convective medium while the other maintains a constant temperature prescribed by the internal body temperature. In Figure 2, Q_{m1} and Q_{m2} denote the normal metabolism and the tumor metabolism respectively.

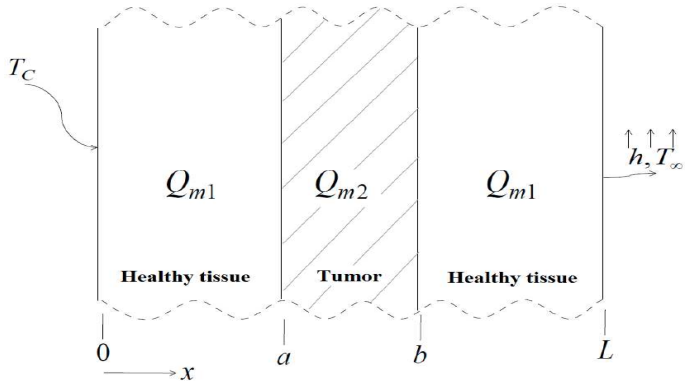

Figure 2. One-dimensional model of three layers of tissue exposed to a convective medium.

Thus, the problem shown in Fig. 2 can be described by the Pennes' equation as

$$\frac{\partial^2 T}{\partial x^2} + w\rho_s c_s(T_a - T) + Q_m = \frac{1}{\alpha}\frac{\partial T}{\partial t} \tag{3}$$

subjected to the boundary conditions, at $x = 0$:

$$T(0, t) = T_a \tag{4}$$

and at x = L

$$-k\frac{\partial T}{\partial x}\bigg|_{x=L} = h(T - T_\infty) \tag{5}$$

and the initial condition

$$T(x,0) = T_a \tag{6}$$

The analytical solution can be obtained by Green's Functions method (Beck *et al.*, 1992). The temperature distribution is obtained as (Figueiredo, 2014)

$$\begin{aligned} T(x,t) = \Bigg\{ & -2(T_0 - T_\infty)\sum_{n=1}^{\infty} e^{\frac{-\beta_n^2\alpha t}{L^2}} \frac{(\beta_n^2 + B^2)\sin(\frac{\beta_n x}{L})[\cos(\beta_n) - 1]}{\beta_n(\beta_n^2 + B^2 + B)} \\ & \frac{-2L^2Q'_{m1}}{k}\sum_{n=1}^{\infty}(e^{m^2\alpha t} - e^{\frac{-\beta_n^2\alpha t}{L^2}})\frac{(\beta_n^2 + B^2)\sin(\frac{\beta_n x}{L})[\cos(\frac{\beta_n a}{L}) - 1]}{\beta_n(\beta_n^2 + B^2 + B)(\beta_n^2 + m^2L^2)} \\ & \frac{-2L^2Q'_{m2}}{k}\sum_{n=1}^{\infty}(e^{m^2\alpha t} - e^{\frac{-\beta_n^2\alpha t}{L^2}})\frac{(\beta_n^2 + B^2)\sin(\frac{\beta_n x}{L})[\cos(\frac{\beta_n b}{L}) - \cos(\frac{\beta_n a}{L})]}{\beta_n(\beta_n^2 + B^2 + B)(\beta_n^2 + m^2L^2)} \\ & \frac{-2L^2Q'_{m1}}{k}\sum_{n=1}^{\infty}(e^{m^2\alpha t} - e^{\frac{-\beta_n^2\alpha t}{L^2}})\frac{(\beta_n^2 + B^2)\sin(\frac{\beta_n x}{L})[\cos(\beta_n) - \cos(\frac{\beta_n b}{L})]}{\beta_n(\beta_n^2 + B^2 + B)(\beta_n^2 + m^2L^2)} \\ & +2(T_c - T_\infty)\sum_{n=1}^{\infty}(e^{m^2\alpha t} - e^{\frac{-\beta_n^2\alpha t}{L^2}})\frac{\beta_n(\beta_n^2 + B^2)\sin(\frac{\beta_n x}{L})}{(\beta_n^2 + B^2 + B)(\beta_n^2 + m^2L^2)}\Bigg\} e^{-m^2\alpha t} + T_\infty \end{aligned} \tag{7}$$

where

$$m^2 = \frac{w\rho_s c_s}{k} \tag{8}$$

5. INVERSE SOLUTION

The function specification method treats the inverse heat conduction problem by assuming a functional variation form of the heat flux. This function can be a sequence of constant segments, line segments or take parabolic, cubic, or exponential forms (Beck *et al.*, 1995). Other possible variations of this method included the simultaneous estimation of all parameters for the whole interval of the field or the sequential estimation of parameters. In this study, the function specification method is used to sequentially estimate the location and intensity of metabolic heat generation in the tumor through Pennes's equation.

To estimate a heat source function varying in space and time, the active surface is broken up into *n* elements, each with a constant heat source component. It is temporarily assumed that the heat source components are constant over *r* future time steps, i.e.,

$$Q_M = Q_{M+1} = \cdots = Q_{M+r-1} \tag{9}$$

The objective function to be minimized in order to estimate Q_M is defined as

$$S = \sum_{i=1}^{r}\left(T^*(t_{M+i-1}) - Y(t_{M+i-1})\right)^2 \tag{10}$$

where T^* and Y are theoretical and simulated/experimental temperatures, respectively, at a point in the body.

6. NUMERICAL RESULTS

The sequential method is used to estimate the location and intensity of metabolic heat generation of the tumor for a 1D case. Table 1 lists the properties used to solve the inverse problem (taken from the simulation study of (Gautherie, 1980), where T_a = 37 ^{O}C, T_∞ = 20^{O}C, and h = 5 W/m^{2}K.

The great difficulty in solving inverse problems with multiple variables is the presence of local minima. In this study, the location and metabolic tumor heat generation are predetermined. A tumor ([a:b]) of 1 cm is assumed to exist within a body of length L = 6 cm, as shown in Fig. 2.

Table 1. Thermal properties of breast (Gautherie, 1980)

Properties	Healthy tissue	Tumor
Thermal conductivity, k	0.42 W/(m K)	0.42 W/(m K)
Blood perfusion, w	0.00018 $1/s$	0.009 $1/s$
Specific mass, ρ	920 kg/m^3	920 kg/m^3
Specific heat, c	3000 J/(kg K)	3000 J/(kg K)
Volumetric heat generation, Q_m	450 W/m^3	29000 W/m^3

Estimating the profile of the metabolic heat generation in the tumor using the sequential function specification method consists of the following steps:

1. Define the properties and the direct problem parameters, including the generation term (size, location and magnitude).
2. Resolve the direct problem using commercial COMSOL software over a time period of 1200 s.
3. Obtain the temperature at x = L shown in Fig. 2.
4. Use the simulated temperatures in the sequential function specification method with 200 future time steps to estimate the magnitude and location of the generation term.
5. Estimate the magnitude of tumor metabolic heat generation assuming that the tumor is at each preset location/interval (0 - 1, 1 - 2, 2 - 3, 3 - 4, 4 - 5, and 5 - 6).
6. As the generation terms are obtained for each assumed preset location, new temperature profiles for the outer surface are calculated using the direct problem.
7. The simulated temperature profile which agrees the best with the temperature profile corresponding to the real location of the tumor is selected.
8. This agreement is verified by calculating Pearson's correlation coefficient between the estimated and simulated temperature profiles (Gibbons and Chakraborti, 2003).
9. Thus, the location and magnitude of the tumor are obtained.

6.1 Body without Tumor

First, the sequential function specification method is executed for a healthy body of 6 cm (i.e., without the presence of an internal tumor, considering only the effect of healthy metabolic heat generation) for 1200 s. After obtaining the simulated temperatures, metabolic heat generation is estimated for six different intervals [a:b] (0 - 1, 1 - 2, 2 - 3, 3 - 4, 4 - 5, and 5 - 6) as the presumed location of the tumor. For each hypothetical interval, a metabolic heat generation profile is generated.

After obtaining the heat generation profiles for each preset location, new profiles of the outer surface temperature (at x = 0.06 m) are calculated. The Pearson's correlation coefficient between the estimated and simulated temperatures are studied.

Pearson's correlation coefficient measures the degree of linear correlation between two quantitative variables. It is a dimensionless ratio ranging from -1.0 and 1.0, and reflects the strength of a linear relationship between two datasets (Gibbons and Chakraborti, 2003).

The correlation between the estimated and simulated temperatures is computed using the MATLAB function "corr". Table 2 presents the results obtained for this study. The correlation between the temperatures obtained in the intervals

[0.03: 0.04] m, [0.04: 0.05] m, and [0.05: 0.06] m had values of 0.9999, with magnitudes of metabolic heat generation being 333, 320 and 384 W/m^3, respectively. These estimated values are approximately equal to the values associated with normal body metabolism (450 W/m^3). This analysis is important in that the heat generation intensity is different from the abnormal heat generation associated with a tumor (29000 W/m^3). Figure 3 compares the simulated and estimated normal metabolic heat generation.

Table 2. Correlation coefficient of the simulated and estimated temperatures for the body without tumor.

Tumor location [a:b]	Estimated heat metabolic W/m^3	Correlation
$[0.00 : 0.01]$ m	-2,544116E+021	0.6508
$[0.01 : 0.02]$ m	5,008781E+019	-0.7093
$[0.02 : 0.03]$ m	3,453237E+006	-0.7626
$[0.03 : 0.04]$ m	3.335232E+002	0.9999
$[0.04 : 0.05]$ m	3.204409E+002	0.9999
$[0.05 : 0.06]$ m	3.840668E+002	0.9999

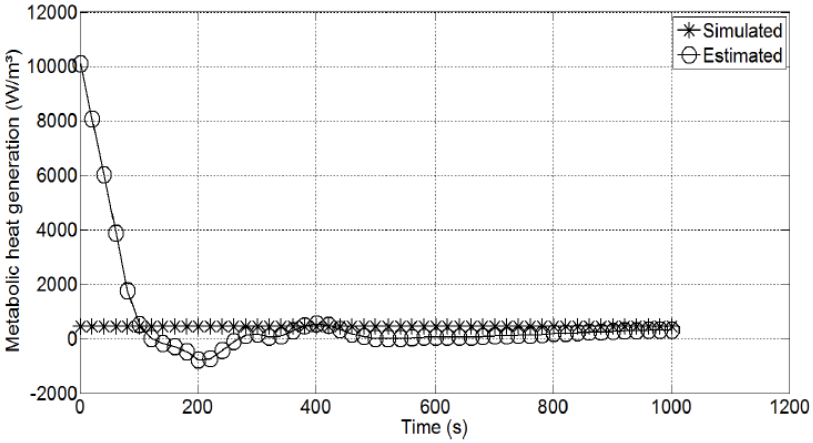

Figure 3. Comparison of the simulated and estimated metabolic heat generation for a body without a tumor.

6.2 Body with Tumor

In the following, is described the analysis of a case where a tumor is located in the interval [0.04: 0.05] m within the body. Using the same procedure as in the previous case, the temperatures at x = L are obtained from the direct problem, and then the metabolic heat generation is estimated using the same six hypothetical location intervals for the tumor.

Table 3 presents the results of the correlation between the simulated temperatures and the temperatures estimated by the sequential function specification method. Pearson's correlation coefficient is 0.9989 for the [0.04: 0.05] m interval. The corresponding metabolic heat generation is 28966 W/m^3, i.e., an error of only 0.1% between the estimated and the simulated metabolic heat generation. Fig. 4 shows a comparison of the simulated and estimated metabolic heat generation.

Table 3. Correlation coefficient of the simulated and estimated temperatures for the body with a tumor located at [0.04: 0.05] m.

Tumor location [a:b]	Estimated heat metabolic W/m^3	Correlation
$[0.00 : 0.01]$ m	-1.390275E+022	-0.8785
$[0.01 : 0.02]$ m	3.070347E+020	0.9176
$[0.02 : 0.03]$ m	1.287933E+010	0.9477
$[0.03 : 0.04]$ m	4.389649E+004	0.9539
$[0.04 : 0.05]$ m	2.896647E+004	0.9989
$[0.05 : 0.06]$ m	.632095E+004	0.8298

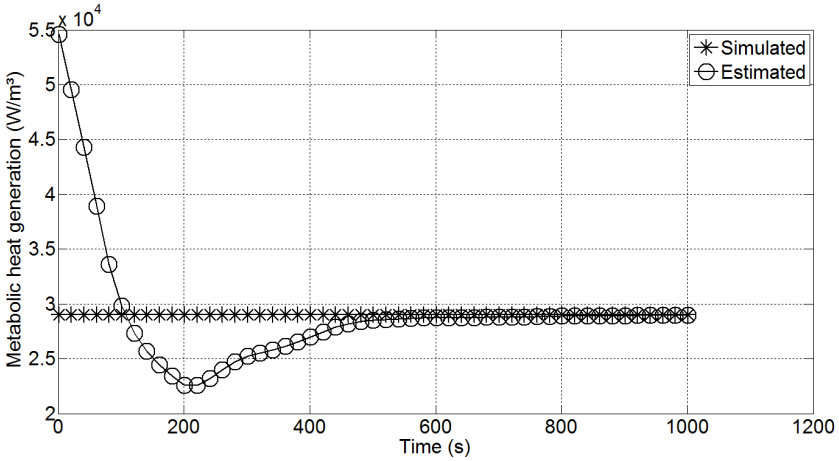

Figure 4. Comparison of the simulated and estimated metabolic heat generation for a tumor located at [0.04: 0.05] m.

The location and magnitude of the metabolic heat generation of the tumor has been determined. However, only six hypothetical intervals of 1 cm were used to obtain the desired profile. Thus, a more refined discretization is proposed. along with a study of the correlation between the simulated and estimated temperatures for a total of 51 possible tumor sites in the body, e.g., [0: 0.01] m, [0.001; 0.011] m, [0.002: 0.012] m, ... [0.049: 0.059] m, and [0.050: 0.060]m. The results obtained from this new analysis demonstrate that the correlation for the interval [0.04: 0.05] m is the best.

7. Experimental Results

Figure 5 illustrates an experiment performed in the laboratory to demonstrate the efficiency of the technique in situ. The experiment is similar to the simulation problems presented in previous sections. Two samples of polyvinyl chloride (PVC) plates (k = 0.15 W/(m K), ρ = 1488 kg/m^3, c = 861 J/(kg K)), with dimensions of 300 x 300 x 25 mm represent the tissue. An electrical resistance of 18 Ω (300 x 300 x 1 mm) is inserted in half of the sample for the generation of heat. The temperature on the lower surface maintained at 37 ^{o}C, using thermostatic bath. The remaining surfaces are exposed to an environment having a convection coefficient equal to 10 W$/\left(\mathrm{m}^2\mathrm{K}\right)$ and an ambient temperature of 25 ^{o}C. As the proposed technique uses the temperature difference between thermal models (with inclusion and without inclusion), neither the blood perfusion nor the metabolic terms in either model have an influence on the results. In this sense, they are not considered in the experimental tests.

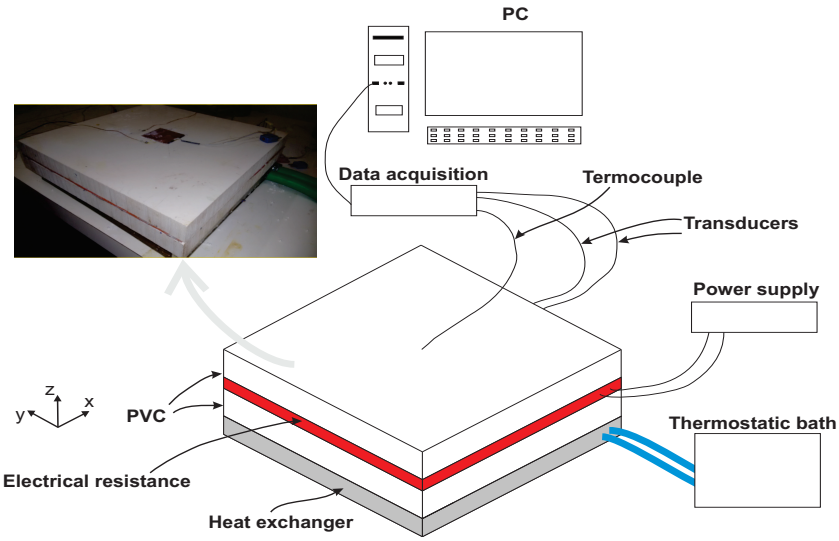

Figure 5. Experimental schematic setup using PVC.

Fig. 6 shows a view of the y-z plane of the experimental model cut at x = 150 mm. A thermocouple, type K, 28AWG, was used to measure the temperature of the upper face exposed to the environment. In Fig. 6, $L = 51$ mm, $a = 25$ mm, and $b = 26$ mm. There are two heat transfer transducers of size 2500 mm^2 placed on the upper and lower surfaces of the electric heater. The signals from these transducers are not used for the estimations, but for a later validation of the technique.

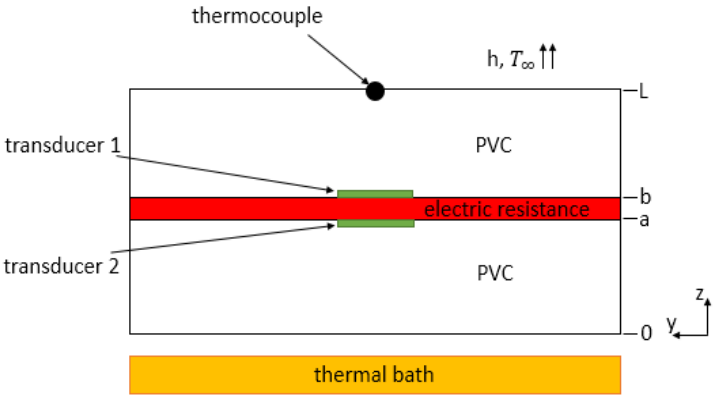

Figure 6. Cut plane yz at x =150 mm of the experiment.

The calibration curve of the transducers is given by $q_1" = 153797U_1 - 20.205$, and $q_2" = 651063U_2 - 20.205$, where $q_1"$ and $q_2"$ [W/m^2] denote the transducers 1 and 2, respectively. U_1 and U_2 are the electric voltage signals [V] of transducers 1 and 2, respectively. It can be observed that the experimental setup contributes strongly of heat only in the direction of the z-axis. This hypothesis can be ensured for the central location of the electric resistance (x = 150 mm, y = 150 mm, z). Thirty experiments with the same configuration were performed in the laboratory. Fig. 7a shows the typical heat flux signals from the transducers during the experiment. A power of 35.79 W (25.38 V of tension) was supplied to the electrical resistance for all 30 runs. Fig. 7b shows the top surface temperature (at x = 150 mmm, y = 150 mm, z = 51 mm) developed during the experiment.

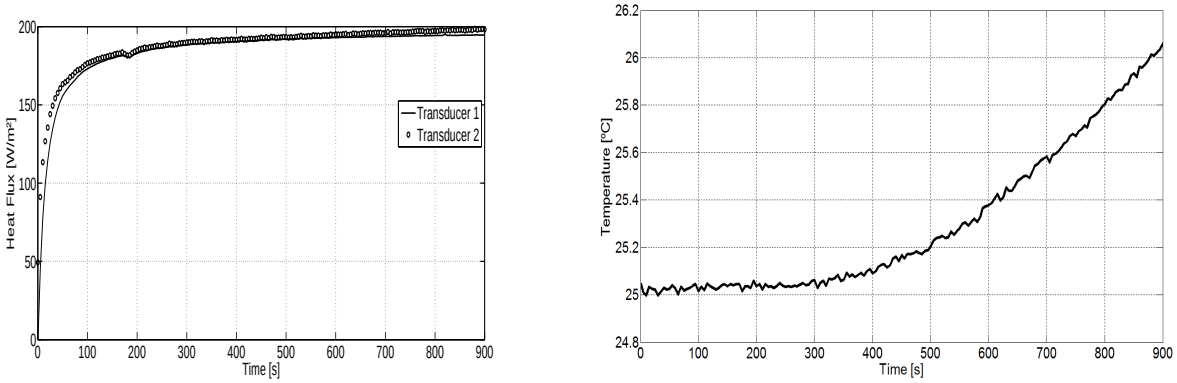

(a) (b)

Figure 7. (a) Heat flux signals of the transducers, (b) Top surface temperature measured during the experimental.

Fig. 8 shows the correlations results between the measured experimental temperatures and calculated temperatures obtained from the theoretical model to determine the location of the heat source in a single experiment. The x-axis represents the 101 different intervals in which the tumor is assumed to be located. The highest correlation obtained in this case was 0.99828 in the interval [24: 25] mm.

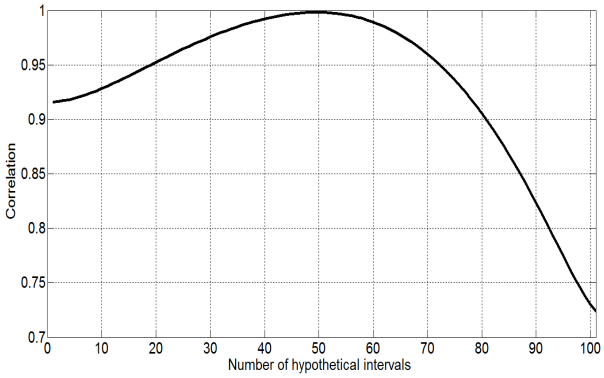

Figure 8. Correlations for all attempts to determine the location of the heat source in the experiment.

The estimated location of the heat source for the 30 experiments is [22.86: 23.86] mm. Thus, the difference between the average estimated location and real location of the source is 8.5%. The estimated volumetric heat generation using the sequential method is 435008.76 W/m^3, which indicates that the volumetric heat flux is 39.15 W, giving rise to an estimated error of 9.4%. Fig. 9 shows the comparison between the experimental temperatures and the temperatures calculated from the estimated mean value of the heat generation.

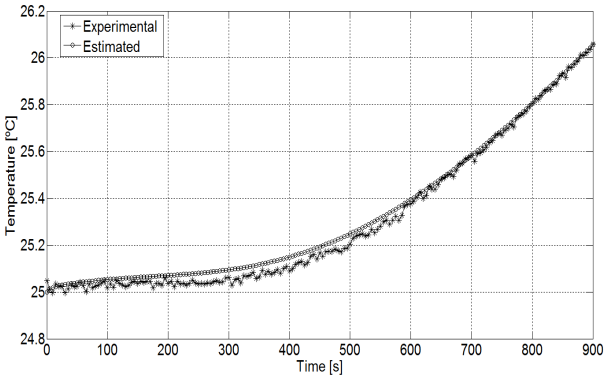

Figure 9. Comparison between estimated and experimental temperatures.

8. Conclusions

The magnitude and location of metabolic heat generation from a simulated tumor have been estimated satisfactory. The results show the ability of the proposed method to identify volumetric heat generation in two tumor tissue problems. The estimates in the simulations were sufficiently accurate for the localization of the tumors and the intensity of the heat source was determined with a maximum error of 0.1%. The experimental results presented estimates for the location and intensity of a heat source for a PVC phantom tissue with error of less than 10%. The proposed method therefore represents an excellent technique for application in both *in vitro* and *in vivo* cases.

9. ACKNOWLEDGEMENTS

The support provided by CNPq, CAPES and FAPEMIG, agencies of the Brazilian government, is greatly appreciated.

10. REFERENCES

Adams, F., 1849. *The Genuine Works of Hippocrates*. W. Wood and Company, London.

Amalu, W.C., Hobbins, W.B., Head, J.F. and Elliot, R.L., 2006. *The Biomedical Engineering Handbook – Medical Devices ans Systems,*. CRC Press.

Beck, J.V., Blackwell, B. and St., Clair, C.R., 1995. *Inverse Heat Conduction: Ill-posed Problems*. Wiley-Interscience, New York, NY.

Beck, J.V., Cole, K.D., Haji-Sheik, A. and Litkouhi, B., 1992. *Heat Conduction Using Green's Function*. Hemisphere Publishing, Washington, DC.

Bezerra, L.A., Oliveira, M.M., Rolim, T.L., Conci, A., Santos, F.G.S., Lyra, P.R.M. and Lima, R.C.F., 2013. "Estimation of breast tumor thermal properties using infrared images". *Signal Processing*, Vol. 93, pp. 2851–2863.

Bhowmik, A. and Repaka, R., 2016. "Estimation of growth features and thermophysical properties of melanoma within 3-d human skin using genetic algorithm and simulated annealing". *International Journal of Heat and Mass Transfer*, Vol. 98, pp. 81–95. doi:doi.org/10.1016/j.ijheatmasstransfer.2016.03.020.

BreastCancer.org, 2017. "Thermography". http://www.breastcancer.org/symptoms/testing/types/thermography.

Charny, C.K., 1992. *Bioengineering Heat Transfer*, Academic Press, Inc, Vol. 22, chapter Mathematical models of bioheat transfer, pp. 19–155.

Chen, M.M. and Holmes, K.R., 1980. "Microvascular contributions in tissue heat transfer". *Annals of the New York Academy of Sciences*, Vol. 335, pp. 137–150. doi:10.1111/j.1749-6632.1980.tb50742.x.

Figueiredo, A.A.A., 2014. *Numerical analysis of thermal models involving the estimation of parameters in bioheat equation.* master's degree, Federal University of Uberlandia - Department of Mechanical Engineering.

Gautherie, M., 1980. "Thermopathology of breast cancer: Measurement and analysis of in vivo temperature and blood flow". *Annals of the New York Academy of Sciences*, Vol. 335, p. 383–415.

GenisisCare, 2018. "Skin cancer". https://www.genesiscare.co.uk/skin-cancer.

Gibbons, J.D. and Chakraborti, S., 2003. *Nonparametric Statistical Inference*. Marcel Dekker, Inc., New York, NY, 4th edition.

Keller, K.K. and Seiler, L., 1971. "An analysis of peripheral heat transfer in man". *Journal of Applied Physiology*, Vol. 30, No. 5, pp. 779–786.

Klinger, H.G., 1978. "Heat transfer in perfused biological tissue – ii. the "macroscopic" temperature distribution in tissue". *Bulletin of Mathematical Biology*, Vol. 40, pp. 183–199.

Mishra, S.C. and Das, K., 2015. "Simultaneous estimation of size, radial and angular locations of a malignant tumor in a 3-d human breast - a numerical study". *Journal of Thermal Biology*, Vol. 52, pp. 147–156.

Mital, M. and Scott, E.P., 2006. "Thermal detection of embedded tumors using infrared imaging". *Journal of Biomechanical Engineering*, Vol. 129, pp. 33–39.

Mitchell, J.W. and Myers, E.G., 1968. "An analytical model of the countercurrent heat exchange phenonena". *Biophysical Journal*, Vol. 8, pp. 897–911.

Nakayama, A. and Kuwahara, F., 2008. "A general bioheat transfer model based on the theory of porous media". *International Journal of Heat and Mass Transfer*, Vol. 51, No. 11, pp. 3190–3199.

of Clinical Thermology, I.A., 2017. "What is breast thermography". http://www.iact-org.org/patients/breastthermography/what-is-breast-therm.html.

Pennes, H.H., 1948. "Analysis on tissue arterial blood temperature in the resting human forearm". *Applied Physiology*, Vol. 1, No. 2, pp. 93–122.

Roetzel, W. and Xuan, Y., 1998. "Transient response of the human limb to an external stimulust". *International Journal of Heat and Mass Transfer*, Vol. 41, No. 1, pp. 229–239.

Sadeghi-Goughari, M., Mojra, A. and Sadeghi, S., 2016. "Parameter estimation of brain tumors using intraoperative thermal imaging based on artificial tactile sensing in conjunction with artificial neural network". *Journal of Physics D: Applied Physics*, Vol. 49, No. 7.

Weinbaum, S. and Jiji, M.L., 1985. "A new simplified bioheat equation for the effect of blood flow on local average tissue temperature". *Journal of Biomechanical Engineering*, Vol. 107, No. 2, pp. 131–139.

11. RESPONSIBILITY NOTICE

The authors are the only responsible for the printed material included in this paper.